Estradiol Enhances Thiazide-sensitive NaCl Cotransporter Density in the Apical Plasma Membrane of the Distal Convoluted Tubule in Ovariectomized Rats

Jill W. Verlander,* Tuan M. Tran,* Li Zhang,* Mark R. Kaplan,‡ and Steven C. Hebert§

**Division of Nephrology, Hypertension, and Transplantation, University of Florida College of Medicine, Gainesville, Florida 32610-0224; ‡Renal Division, Brigham and Women's Hospital, Boston, Massachusetts 02115; and §Division of Nephrology, Vanderbilt University Medical Center, Nashville, Tennessee 37232*

Abstract

Recent data suggest that sex hormones affect the thiazide-sensitive NaCl cotransporter (TSC) density or binding capacity (Chen, Z., D.A. Vaughn, and D.D. Fanestil. 1994. *J. Am. Soc. Nephrol.* 5:1112–1119). Thus, we determined the effect of ovariectomy (OVX) and estrogen replacement on the ultrastructural localization of TSC in rat kidney using immunocytochemistry.

Kidneys of intact female (CON) and OVX rats fed ad libitum for 6 and 9 wk or pair-fed for 9 wk were processed for transmission electron microscopy. Immunogold localization of rat TSC (rTSC1) demonstrated intense label in the apical plasma membrane of CON distal convoluted tubule (DCT). In OVX DCT, rTSC1 label and apical plasma membrane microprojections were decreased. Western blots of renal membrane protein from pair-fed CON and OVX revealed bands at 129–135 kD, but the OVX signal was reduced. Morphometric analyses demonstrated that injecting 10 μg/kg body weight 17β-estradiol subcutaneously 4×/wk in OVX rats restored DCT apical microprojections and label density for rTSC1.

Thus, in OVX rats (*a*) rTSC1 immunoreactive renal membrane protein is reduced; (*b*) apical plasma membrane complexity and immunogold label for rTSC1 in DCT is decreased; and (*c*) estradiol replacement restores DCT ultrastructure and rTSC1 label to normal. We conclude that estrogen enhances the density of rTSC1 in the DCT, and may alter renal Na transport by this mechanism. (*J. Clin. Invest.* 1998. 101:1661–1669.) Key words: estradiol • distal tubule • thiazide diuretics • kidney ultrastructure • immunohistochemistry

These studies were presented in part at the combined Annual Meetings of the Southern Section of the American Federation for Clinical Research and the Southern Society for Clinical Investigation in New Orleans, LA, January 31–February 3, 1996, and at the Annual Meeting of the American Society of Nephrology in New Orleans, LA, in November, 1996, and have been published in abstract form (*J. Investig. Med.* 1996. 44:49*a*; and *J. Am. Soc. Nephrol.* 1996. 7:1293).

Address correspondence to Dr. Jill W. Verlander, Division of Nephrology, Hypertension, and Transplantation, University of Florida College of Medicine, P.O. Box 100224 Health Science Center, Gainesville, FL 32610-0224. Phone: 352-846-0820; FAX: 352-392-3581; E-mail: verlaj@medicine.ufl.edu

Received for publication 9 May 1997 and accepted in revised form 13 February 1998.

J. Clin. Invest.

0021-9738/98/04/1661/09 $2.00
Volume 101, Number 8, April 1998, 1661–1669
http://www.jci.org

Introduction

Although it has been known for many years that estrogen can reduce renal sodium excretion (1), the precise mechanism responsible for this effect is not known. Because orally administered estrogens have been shown to increase plasma angiotensinogen and plasma renin activity (3), sodium retention observed with acute estrogen administration has been attributed to activation of the renin–angiotensin system. However, the effect of estrogen on the kidney has not been specifically determined.

Recently Chen et al. (2) have demonstrated that in rats, ovariectomy reduces binding of tritiated metolazone, an analog of thiazide diuretics, in renal homogenates. These data suggest that sex hormones may regulate either the density or the binding capacity of thiazide receptors in the kidney. Thiazide diuretics bind to and inhibit the thiazide-sensitive NaCl cotransporter (TSC),[1] which is located primarily in the distal convoluted tubule where it mediates apical NaCl uptake (4). The thiazide-sensitive NaCl cotransporter has been cloned from rat kidney and designated rTSC1 (5). Plotkin et al. (6) have raised a polyclonal antibody against a 110–amino acid peptide from the amino terminus of the transporter, and have used immunocytochemical methods in rat kidney to localize the rTSC1 in the apical plasma membrane of the distal convoluted tubule and in a small subpopulation of cells in the connecting segment.

Based on the knowledge that estrogen can enhance sodium retention, and that ovariectomy reduces thiazide binding in the kidney, we hypothesized that one mechanism by which estrogen may alter renal sodium handling is by regulating the TSC in the distal convoluted tubule. In the present study, we determined the effect of ovariectomy and estrogen replacement on the location and density of the thiazide-sensitive NaCl cotransporter in the rat distal convoluted tubule using the anti-rTSC1 antibody, immunogold cytochemistry, transmission electron microscopy, and morphometric analysis.

Methods

Animals. Female Sprague-Dawley rats (Harlan Sprague Dawley, Inc., Indianapolis, IN) weighing 180–200 g were fed standard rat chow (Laboratory Rodent Diet 5001; PMI Feeds, Inc., St. Louis, MO) and housed in the Animal Resources Division at the University of Florida Health Science Center for 1 wk before undergoing surgical proce-

1. *Abbreviations used in this paper:* CON, intact female; DCT, distal convoluted tubule; OVX, ovariectomized; OVX-EST, ovariectomized rat treated with estradiol; OVX-VEH, ovariectomized rat treated with vehicle; rTSC1, thiazide-sensitive NaCl cotransporter cloned from rat renal cortex; SHAM-VEH, sham-operated rat treated with vehicle; TSC, thiazide-sensitive NaCl cotransporter.

dures. For the initial experiments, animals either were left intact or were anesthetized with 50 mg/kg body wt ketamine HCl and 10 mg/kg body wt xylazine intraperitoneally, and underwent bilateral ovariectomy. After surgery, animals either were fed ad libitum or were pair-fed to control sodium intake. For pair feeding, intact female (CON) and ovariectomized (OVX) rats were matched by weight before the ovariectomy, and the food given to each OVX rat was limited to the amount consumed by the CON rat in each pair.

In additional experiments, rats were anesthetized as described, and were subjected to either bilateral ovariectomy, or were sham-operated. In these experiments, a group of ovariectomized animals (OVX-EST) received subcutaneous injections of 10 μg/kg BW 17β estradiol in 1% benzyl alcohol in corn oil four times weekly. The sham-operated animals (SHAM-VEH) and a separate group of ovariectomized animals (OVX-VEH) received vehicle injections only.

Physiology. 8 wk after surgery, food was withheld, and 24-h urine samples were collected for determining urinary sodium excretion. Urine sodium concentrations were determined using a model 643 flame photometer (Instrumentation Laboratory, Inc., Lexington, MA).

Tissue processing. For initial observations 6 and 9 wk after surgery, CON ($n = 3$) and OVX ($n = 6$) rats fed ad libitum were anesthetized with 50 mg/kg body wt pentobarbital sodium intraperitoneally, and the kidneys were preserved by in vivo perfusion with periodate-lysine-2% paraformaldehyde (7) followed by overnight immersion at 4°C or 1% glutaraldehyde in Tyrode's buffer, followed by a 2–4-h immersion in the same fixative. The kidneys of pair-fed CON ($n = 6$), OVX ($n = 4$), SHAM-VEH ($n = 3$), OVX-VEH ($n = 4$), and OVX-EST ($n = 4$) animals were preserved by in vivo perfusion with 1% glutaraldehyde 9–10 wk after ovariectomy. Glutaraldehyde-fixed tissue was rinsed overnight in Tyrode's buffer at 4°C. Samples of outer and inner cortex were immersed in 100 mM NH_4Cl for 1 h at 4°C. The tissue samples were then dehydrated in a graded series of alcohols, processed, and embedded in Lowicryl K4M (Chemische Lowi Werke, Waldkraiburg, Germany). Lowicryl polymerization was carried out under ultraviolet light for 24 h at −20°C, and then for 48 h at room temperature. Samples containing well-preserved distal nephron and collecting duct were selected after light microscopic examination of 1-μm-thick sections stained with toluidine blue. Ultrathin sections of these samples were mounted on Formvar/carbon-coated nickel grids for immunogold cytochemistry.

Antibody. The primary antibody was a polyclonal antibody raised in rabbit against a 110–amino acid segment comprising most of the amino terminus of rTSC1. The rabbits were immunized with a synthetic peptide (amino acids 2–112 of rTSC1) fused to maltose binding protein. This antibody has been characterized and used for immunolocalization of the rTSC1 in normal rat kidney (6).

Immunogold labeling. The immunogold labeling procedure was similar to that used previously (8). The following solutions were used: buffer 1: 10 mM tris(hydroxymethyl)aminomethane (Tris) HCl, 500 mM NaCl, 0.025% NaN_3, 1% BSA or ovalbumin, pH 7.2; buffer 2: 10 mM Tris HCl, 150 mM NaCl, 0.025% NaN_3, 0.02% Carbowax PEG 20M (polyethylene glycol with an average of 20 kD; Fisher Scientific, Springfield, NJ) pH 7.2; and buffer 3: 10 mM Tris HCl, 150 mM NaCl, pH 7.2. The primary antibody was diluted 1:100–1:500 in buffer 1. The secondary antibody was goat anti–rabbit IgG conjugated to 15-nm diameter colloidal gold particles (AuroProbe EM™, Amersham Corp., Arlington Heights, IL) diluted 1:50 in buffer 2.

The labeling procedure was performed at room temperature by floating the grids on droplets unless noted otherwise. The grids were treated with fresh 100 mM NH_4Cl for 1 h, rinsed with buffer 3, and then treated with buffer 1 for 30 min. They were partially dried and exposed to the primary antibody overnight at 4°C in a moist chamber. The grids were rinsed with buffer 3 for 30 min, and then treated with buffer 2 for 30 min. They were partially dried, exposed to the secondary antibody for 1 h, rinsed with buffer 3 for 20 min, and then rinsed with a distilled water spray for 30 s. The grids were then counterstained with saturated uranyl acetate and lead citrate. Each group of grids subjected to the immunogold procedure included a control grid that was exposed to preimmune serum or buffer 1 in place of the primary antibody.

Electron microscopy. Ultrathin sections were examined using an EM10™ transmission electron microscope (Carl Zeiss, Inc., Thornwood, NY). The distal convoluted tubule was identified by its characteristic morphology, that is, a tall, homogeneous, cuboidal epithelium exhibiting extensive basolateral plasma membrane infoldings with vertically arrayed mitochondria interspersed among the basolateral plasma membrane infoldings, and an apically situated nucleus.

Morphometric analysis. Amplification of the apical plasma membrane of distal convoluted tubule (DCT) cells and the amount of gold label along the apical plasma membrane were quantified in SHAM-VEH ($n = 3$), OVX-VEH ($n = 4$), and OVX-EST ($n = 3$) rats. Profiles of DCT that included transitions to either the thick ascending limb of the loop of Henle or the connecting segment were excluded from the analysis. Six cells in the DCT of each animal were selected in a random manner by an observer blinded to the experimental conditions using a predetermined progression through the grid, supporting randomly oriented ultrathin sections (9). Alternating cells in each DCT were photographed, beginning with the cell located at the 12 o'clock position, and proceeding clockwise until three cells per profile were photographed. Cells were photographed at 7,800×. At least two tissue blocks per animal were examined, and final selection of photomicrographs to be used for morphometric analysis was done by selecting the first cells photographed in each individual tubule in order of photographing, then the second cells photographed in each tubule, and so on until six micrographs were selected. Individual photomicrographs were examined at a final magnification of ~ 20,300×. The exact magnification was calculated using a calibration grid with 2160 lines/mm.

The amplification of the apical plasma membrane was assessed by determining the boundary length of the apical plasma membrane within a proscribed distance along the apical surface of the cell. Specifically, the apical surface was marked at the first tight junction on the micrograph, and at a point along the apical plasma membrane scribed with a protractor set at a radius of 10 cm, corresponding to 4.93 μm. The observer was blinded to the experimental condition, and the individual photomicrographs were mixed so that the data collection occurred in random order. Using standard morphometric procedures (9), the boundary length of the apical plasma membrane between these points was determined by intersection counting using the Merz curvilinear test grid with a distance of 20 mm between the points corresponding to 0.986 μm (d).

The formula for determining the boundary length (B) using the Merz curvilinear test grid was calculated from the equation $B_A = (\pi/2)I_L$, where B_A = the profile boundary length within the test area A, or B/A, and I_L = the number of intersections of the boundary with the test line L, or I/L. On the Merz grid, $A = P \times d^2$ and $L = P \times (\pi/2) \times d$, where P is the number of points in the test area, and d is the distance between points (9). By substituting for A and L in the formula, $B_A = (\pi/2)I_L$ and solving for B, using the Merz curvilinear test grid,

$$B = I \times d$$

where I represents the number of intersections between the test line and the plasma membrane, and d is the distance between points. B was expressed in microns.

Preparation of samples for Western blot analysis. 9 wk after surgery, pair-fed CON ($n = 4$) and OVX ($n = 4$) rats were anesthetized with 50 mg/kg body wt Na pentobarbital intraperitoneally, and the kidneys were rinsed briefly by retrograde perfusion with PBS through the abdominal aorta. In initial experiments, the kidneys were removed, quickly frozen in liquid nitrogen, and then transferred to a −70°C freezer. In later experiments, the kidney cortex was dissected on ice, and then frozen in liquid nitrogen and transferred to a −70°C freezer. Samples of renal cortex were homogenized in ice-cold buffer composed of 250 mM sucrose, 150 mM NaCl, 30 mM Tris (pH 7.5),

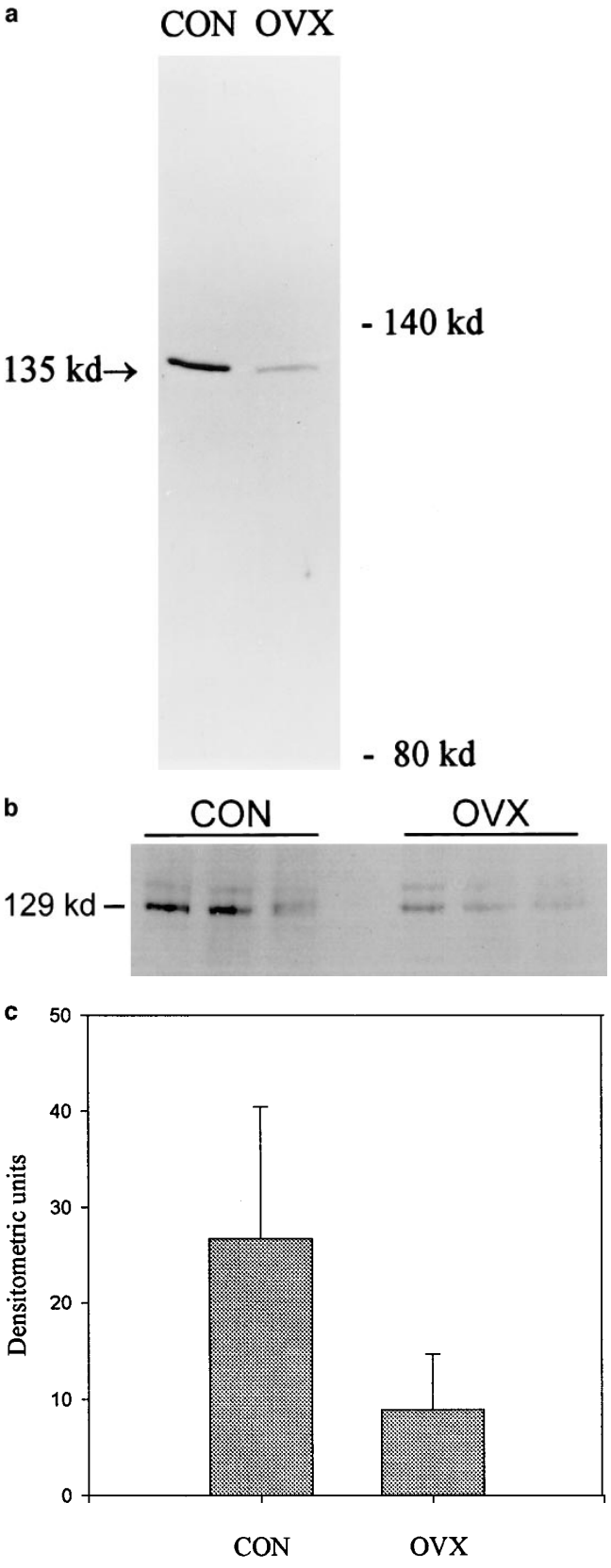

Figure 1. (*a*) Western analysis of rTSC1 immunoreactive renal cortical membrane protein (80 μg/lane) from pair-fed CON and OVX rats using 6% SDS-PAGE and probed with the anti-rTSC1 immune serum diluted 1:400. A single band is evident at ~ 135 kD in both CON and OVX, but the intensity is markedly reduced in OVX (55% of CON). (*b*) Western analysis of rTSC1 immunoreactive renal cortical membrane protein (50 μg/lane) from additional pair-fed CON ($n = 3$) and OVX ($n = 3$) rats using 6% SDS-PAGE. Two bands are present, with the major band at ~ 129 kD. The mean densitometric value for OVX was 33.4% of the mean CON value. (*c*) Histogram illustrating the mean densitometric values and standard deviations of the immunoblot illustrated in *b*.

and 0.5 mM PeFabloc (a protease inhibitor; Boehringer Mannheim Biochemicals, Indianapolis, IN). Homogenates of the renal cortex were centrifuged at 3,000 rpm (1,500 *g*) for 15 min at 4°C to remove the nuclei and cellular debris. The supernatants were collected, and a second protein extraction was performed by resuspending the pellets in homogenization buffer and by repeating the centrifugation as described. The resulting supernatants from the two extractions were combined, and were then separated into a crude membrane fraction and a cytosolic fraction by centrifugation at 45,000 rpm for 1 h at 4°C in an ultracentrifuge (Beckman Instruments, Inc., Fullerton, CA) using a fixed angle rotor, 70.1. Protein concentrations in the samples were determined using the BCA Protein Assay Reagent (Pierce Chemical Co., Rockford, IL) with BSA as a standard.

Electrophoresis and immunoblotting. Crude membrane proteins from CON and OVX rats were separated by SDS PAGE. Different amounts of protein varying from 20 to 80 μg from each sample were dissolved in sample buffer, resolved on a 6% SDS-polyacrylamide gel, and electrophoretically transferred to nitrocellulose membranes (Hybond ECL™; Amersham Corp.). The nitrocellulose membranes were stained with Ponceau S and examined to confirm uniform protein loading of the lanes. After being destained in distilled water, the membranes were quenched in blocking solution (5% nonfat dried milk, 10 mM Tris, pH 7.5, 100 mM NaCl, and 0.1% Tween 20) and incubated overnight with the antibody to rTSC1, diluted 1:400 in the blocking solution. The bound antibody was detected by the enhanced chemiluminescence procedure (Amersham Corp.) using horseradish peroxidase–conjugated goat anti–rabbit IgG diluted 1:10,000 in blocking solution as the secondary antibody. Densitometric analyses were performed on a Power Macintosh computer using the NIH Image 1.60 software.

Statistical analyses. The statistical significance of differences between group means for the morphometric data was determined using one-way ANOVA followed by Bonferroni and Student-Newman-Keuls modified *t* tests. Differences in means with $P < 0.05$ were considered statistically significant. Values were expressed as means±SD.

Results

Physiology. 8 wk after ovariectomy, OVX animals fed ad libitum exhibited a significant increase in body wt compared with CON (CON, 261.5±19.6 vs. OVX, 332.2±32.6 g, $P < 0.05$). A significant difference in body weight was also present in CON and OVX rats that were pair-fed, although the numerical difference between the mean values was not as great as that in the CON and OVX rats fed ad libitum (pair-fed CON, 248.3±14.5 vs. pair-fed OVX, 273.2±6.7 g, $P < 0.05$).

In pair-fed rats, urinary Na excretion rates ($U_{Na}V$) were CON ($n = 9$), 176.0±68.1 vs. OVX ($n = 8$), 205.9±81.0 μEq/24 h/100 g body wt, P = NS. When the $U_{Na}V$ of the SHAM-VEH, OVX-VEH, and OVX-EST animals were compared, there were no significant differences among the groups (SHAM-VEH [$n = 5$], 217.7±85.3; OVX-VEH [$n = 6$], 236.5±64.9; OVX-EST [$n = 6$], 190.6±58.8 μEq/24 h/100 g body wt, P = NS).

Western analysis. When probed with the anti-rTSC1 antibody, Western blots of renal membrane protein from the ini-

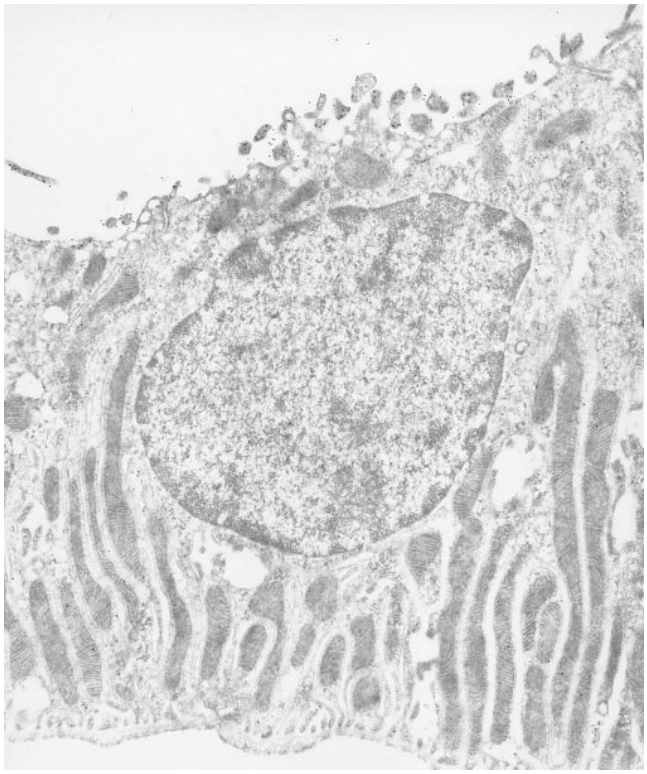

Figure 2. Transmission electron micrograph of a typical distal convoluted tubule cell from a pair-fed CON rat, illustrating the characteristic morphologic features. The distal convoluted tubule is a homogeneous segment composed of tall, cuboidal epithelial cells that contain extensive basolateral plasma membrane infoldings, long, vertically oriented mitochondria that are regularly spaced between the basolateral plasma membrane infoldings, an apically situated nucleus, moderate apical plasma membrane microprojections, and few apical cytoplasmic vesicles. 9,600×.

tial pair of pair-fed CON and OVX rats revealed a band at ~ 135 kD, an appropriate molecular weight for rTSC1 (6). However, the intensity of the band was markedly reduced in the protein extracted from the OVX rats when compared with CON (Fig. 1 *a*). Western blots of renal membrane protein from additional pair-fed CON (n = 3) and OVX (n = 3) rats revealed two bands, with the major band located at ~ 129 kD, and a weaker band at ~ 135 kD (Fig. 1 *b*); the finding of a pair of bands at approximately these molecular weights is consistent with previous studies (6). By densitometry, the intensity of the band in the initial OVX animal was found to be 55% that of CON. In the additional studies, the densitometric values were CON, 26.73±13.69 U vs. OVX, 8.93±5.74 U (Fig. 1 *c*); in this group, OVX was 33.4% of CON. Examination of the Ponceau S–stained nitrocellulose membrane after protein transfer confirmed that the lanes were loaded uniformly with protein.

Immunogold localization of rTSC1. Ultrastructural preservation of the DCT in all animals was excellent, and the morphology of the DCT in CON and SHAM-VEH rats was consistent with previous observations of the DCT in normal rats. The DCT cells were tall cuboidal epithelial cells with numerous vertically arrayed mitochondria, deep infoldings of the basolateral plasma membrane, an apical nucleus, moderately abundant apical plasma membrane microprojections, and a small population of subapical cytoplasmic vesicles (Fig. 2). Immunogold cytochemistry demonstrated that the ultrastructural location of the rTSC1 in both ad libitum- and pair-fed CON rats, as well as in the SHAM-VEH animals, was consistent with the location reported previously in normal rats (6). That is, the rTSC1 immunoreactivity was primarily located along the apical plasma membrane of the DCT (Figs. 3 *a*, 4 *a,* and 5 *a*). In addition, a small population of subapical cytoplasmic vesicles was labeled (Figs. 3 *a*, 4 *a,* and 5 *a*).

In the DCT of both ad libitum and pair-fed OVX rats and in OVX-VEH rats, there was a marked reduction in the number of apical plasma membrane microprojections, as well as a

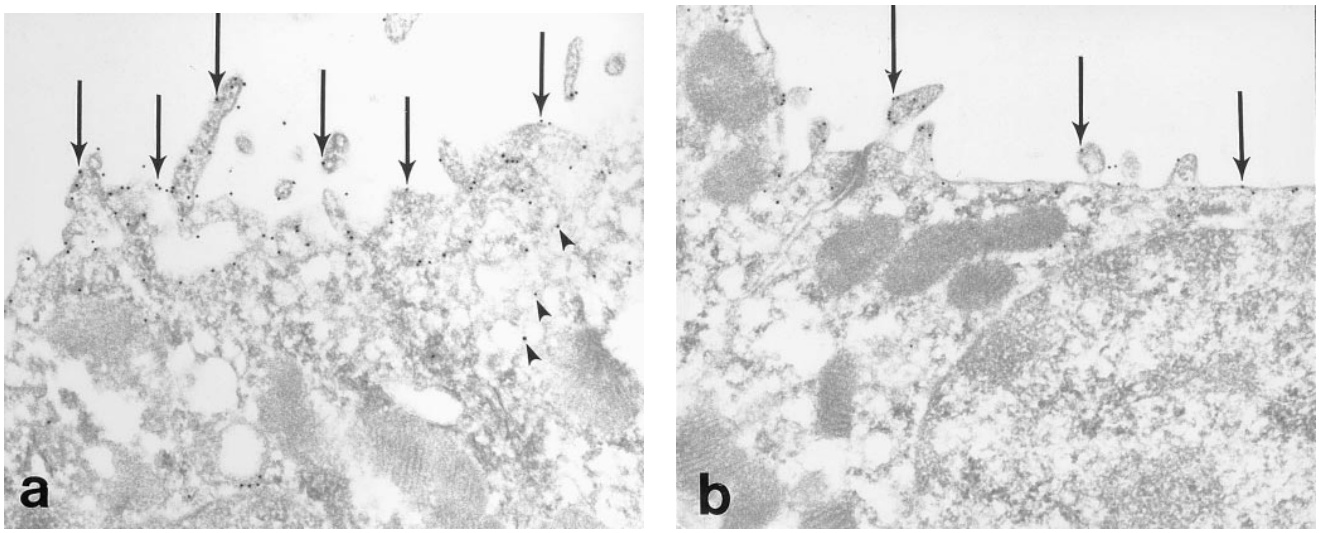

Figure 3. Transmission electron micrographs of the apical region of DCT cells labeled for rTSC1 from CON and OVX rats fed ad libitum for 6 wk before preservation of the kidneys with PLP-fixative. (*a*) CON. There are numerous apical plasma membrane microprojections, and immunogold label is intense along the apical plasma membrane (*arrows*). Occasional gold particles are located on the membrane of apical cytoplasmic vesicles (*arrowheads*). (*b*) OVX. Compared with CON, there is a marked reduction in the number of apical plasma membrane microprojections as well as the number of gold particles along the apical plasma membrane (*arrows*). 22,800×.

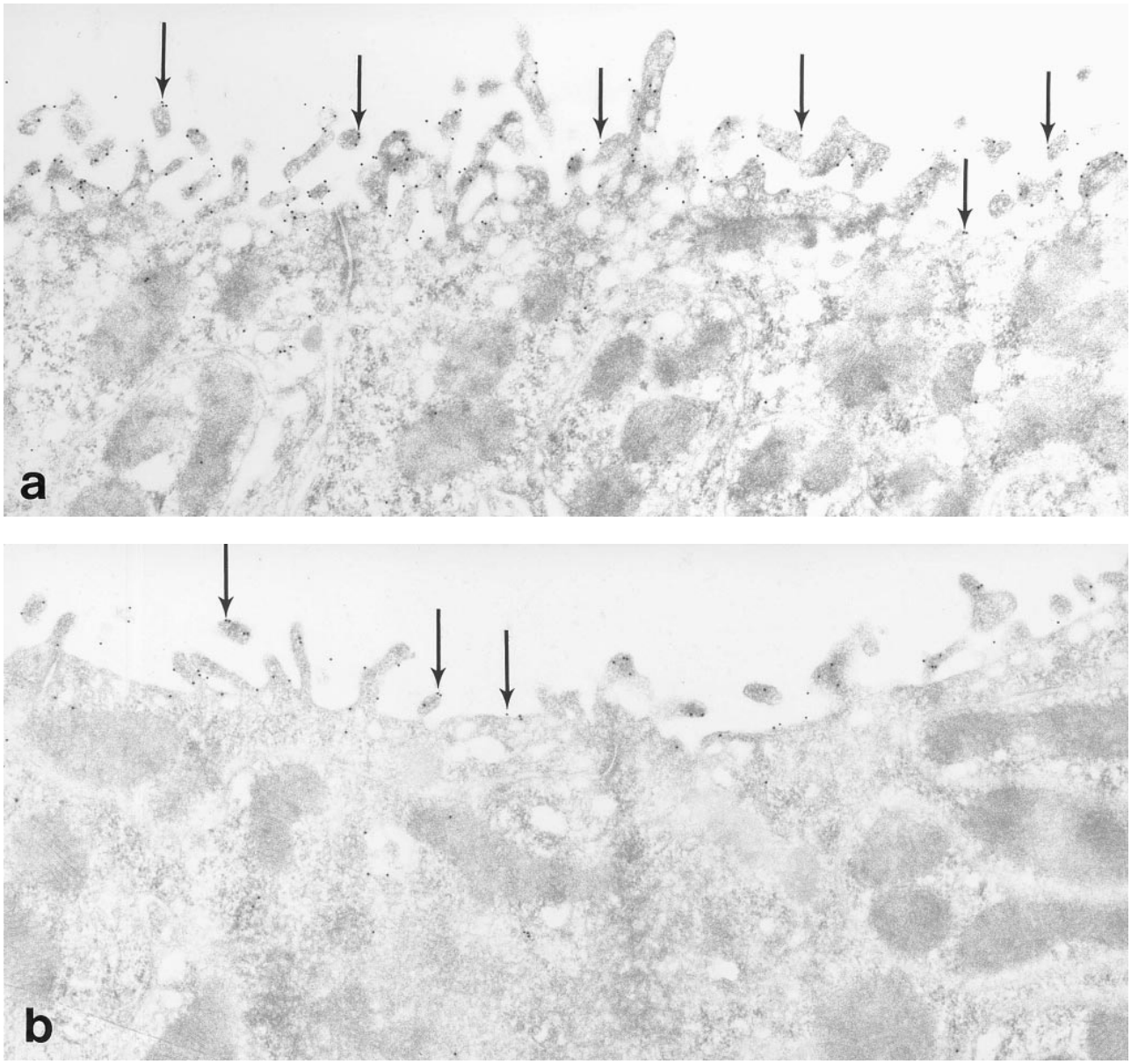

Figure 4. Transmission electron micrographs of the apical region of DCT cells labeled for rTSC1 from CON and OVX rats pair-fed for 9 wk before preservation of the kidneys with 1% glutaraldehyde. (*a*) CON. The apical plasma membrane is densely labeled with gold particles (*arrows*), and there are numerous apical plasma membrane microprojections. (*b*) OVX. As in the OVX rat fed ad libitum, the DCT cell exhibits a marked reduction in apical plasma membrane microprojections and label for the rTSC1 (*arrows*). 22,200×.

decrease in the number of gold particles along the apical plasma membrane (Figs. 3 *b*, 4 *b,* and 5 *b*). There was no apparent change in the number or morphology of the subapical cytoplasmic vesicles or gold label associated with intracytoplasmic structures.

In rats receiving replacement estradiol, the apical plasma membrane of the DCT cells exhibited prominent microprojections and intense gold label for rTSC1 (Fig. 5 *c*). There was no apparent difference in the cytoplasmic vesicle compartment compared with either the SHAM-VEH or OVX-VEH rats.

Morphometric analysis. Quantitation of the boundary length of the apical plasma membrane within a fixed span along the apical surface of DCT cells demonstrated that estradiol replacement in ovariectomized rats resulted in an increase in the complexity of the apical plasma membrane of the DCT when compared with OVX-VEH animals (Fig. 6 *a*). Furthermore, the immunogold label for rTSC1 was diminished in OVX-VEH rats compared with either SHAM-VEH or OVX-EST rats in both the density of label per unit of membrane length (Fig. 6 *b*) and the total number of gold particles along the measured membrane (SHAM-VEH, 68±11.6 vs. OVX-VEH, 31.5±12.3 vs. OVX-EST, 104.6±28.2 colloidal gold particles; $P < 0.05$ for OVX-VEH vs. both SHAM-VEH and OVX-EST).

Controls. In sections subjected to the immunogold procedure with either buffer 1 or preimmune serum substituted for

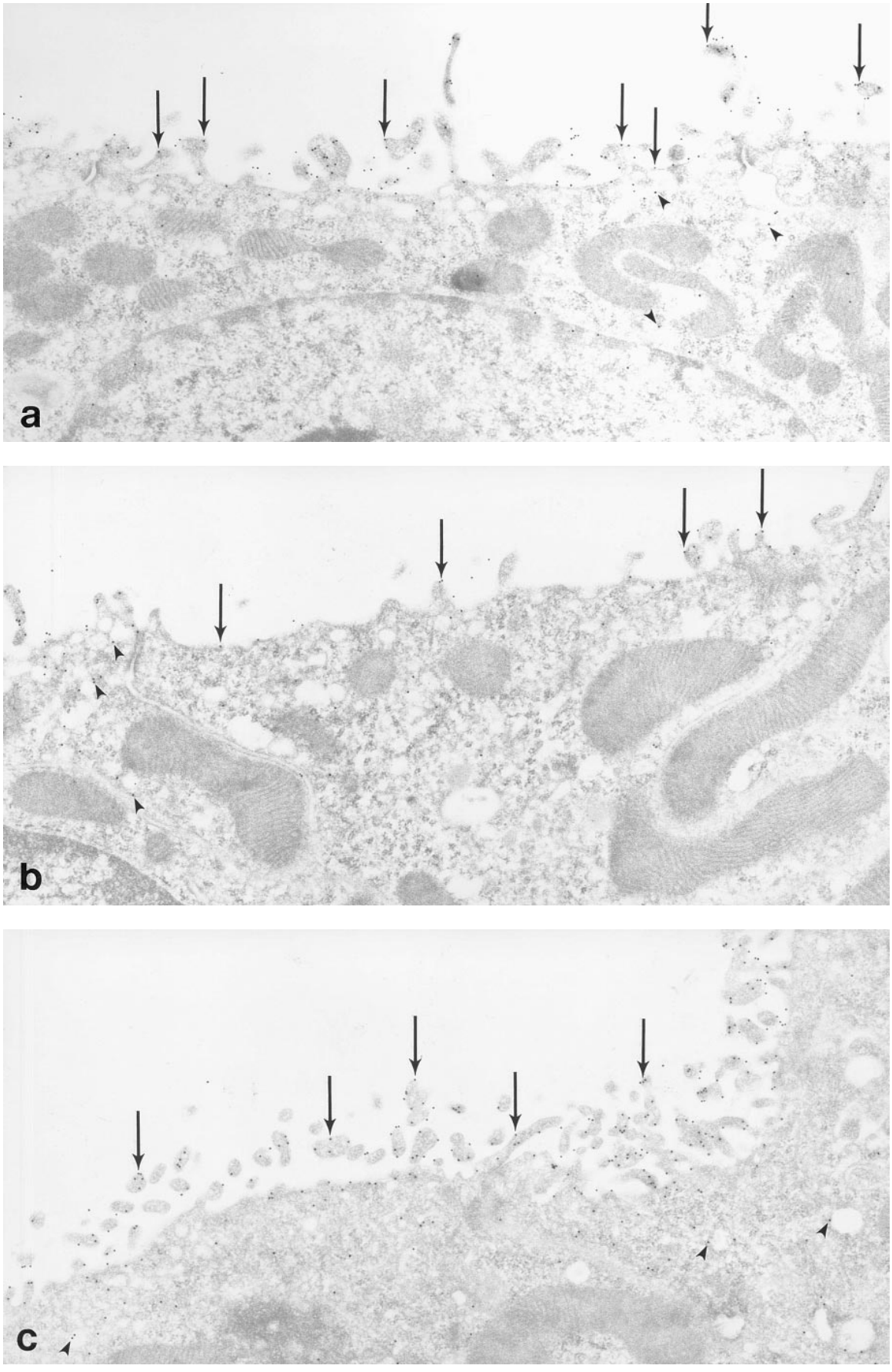
a
b
c

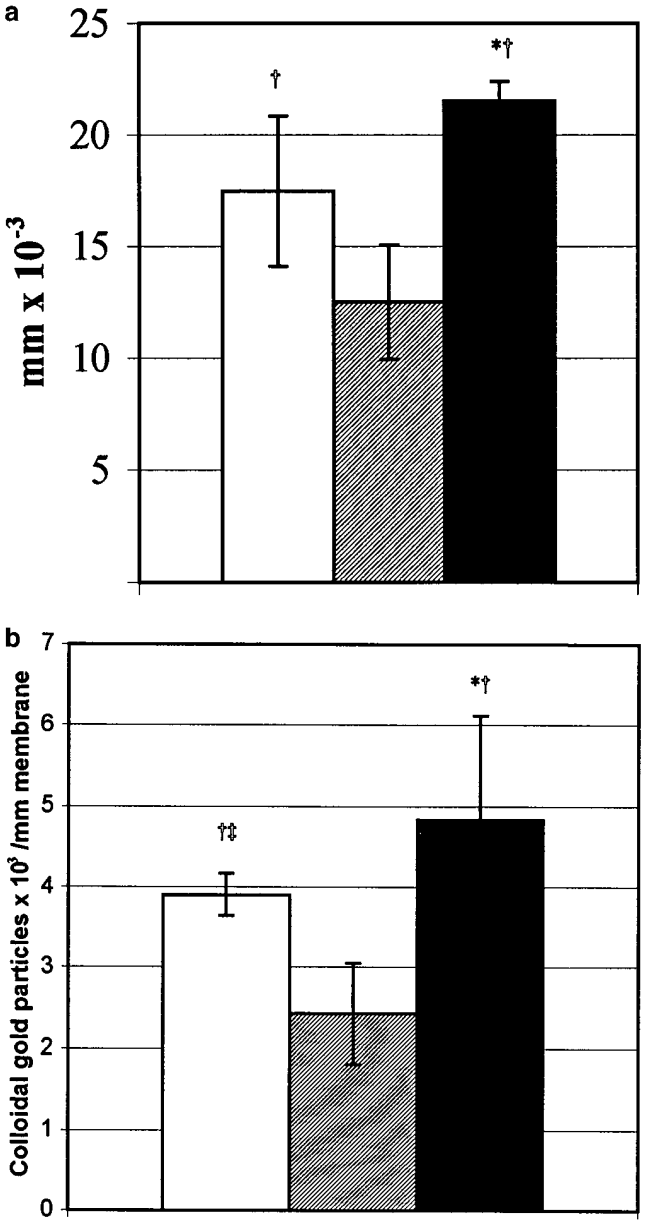

Figure 6. (*a*) Histogram illustrating the results of morphometric analysis of apical plasma membrane boundary length in SHAM-VEH, OVX-VEH, and OVX-EST. The boundary length of the apical plasma membrane within a fixed span of the apical surface of DCT cells was significantly increased in OVX-EST rats compared with OVX-VEH rats, indicating that the number or length of apical plasma membrane microprojections in DCT cells was significantly increased by estradiol replacement. (*b*) Histogram illustrating the results of morphometric analysis of immunogold labeling for TSC along apical plasma membrane in SHAM-VEH, OVX-VEH, and OVX-EST. The density of immunogold label for rTSC1 in the apical plasma membrane of DCT cells was significantly higher in both SHAM-VEH and OVX-EST rats compared with OVX-VEH rats. Statistical analysis was by one-way ANOVA followed by modified *t* tests. Differences between mean values were considered statistically significant when $P < 0.05$. *Different from OVX-VEH by Bonferroni *t* test; †different from OVX-VEH by Student-Newman-Keuls *t* test; ‡different from OVX-EST by Student-Newman-Keuls *t* test. *White bars,* SHAM-VEH; *gray bars,* OVX-VEH; *black bars,* OVX-EST.

the primary antibody, only rare gold particles were evident over the DCT cells (Fig. 7 *a*). In sections subjected to the immunogold procedure including the primary antibody, cells in nephron segments that do not contain rTSC1, such as proximal tubule and thick ascending limb, exhibited only scattered gold particles (Fig. 7 *b*).

Discussion

We have demonstrated that chronic changes in systemic estrogen status in the rat alter both the complexity of the apical plasma membrane as well as the density of the thiazide-sensitive NaCl cotransporter in the apical plasma membrane of the distal convoluted tubule. A decrease in the amount of apical plasma membrane and a decrease in label for rTSC1 was observed in all groups of estrogen-deprived ovariectomized rats compared with intact females, whether fed by free choice or pair-fed. These observations were consistent with our findings of diminished rTSC1 immunoreactivity in renal membrane protein of pair-fed ovariectomized rats compared with the control animals. These findings are also consistent with the data of Chen et al. (2), which demonstrated diminished binding of tritiated metolazone in renal homogenates of ovariectomized rats 6 wk after surgery compared with that found in renal homogenates from intact females.

In addition, we found that estrogen replacement with 17β-estradiol restored both the normal complexity and rTSC1 immunoreactivity to the apical plasma membrane of ovariectomized rats. These observations were confirmed by morphometric analyses that demonstrated a significant increase in amplification of the apical plasma membrane, total amount of immunogold label, and the label density for rTSC1 along the membrane of estradiol-treated OVX rats when compared with vehicle-treated OVX rats. No difference was apparent in the subcellular location of the rTSC1 among any of the conditions.

The mechanisms by which ovariectomy and administration of 17β-estradiol affect the density of the rTSC1 in the distal convoluted tubule have not been determined in this study. Although a direct effect of estrogen on the distal convoluted tubule cells is possible, the presence of estrogen receptors in epithelial cells of the distal nephron has not been reported. However, estrogen is known to increase the circulating levels of a number of hormones that may mediate the effect of estro-

Figure 5. Transmission electron micrographs of the apical region of DCT cells labeled for rTSC1 from SHAM-VEH, OVX-VEH, and OVX-EST rats 9 wk after surgery (*arrows*, gold label along apical plasma membrane; *arrowheads*, gold label associated with cytoplasmic vesicles). (*a*) SHAM-VEH. The normal DCT morphology and immunogold label is evident. (*b*) OVX-VEH. The complexity of the apical plasma membrane and intensity of immunogold label is markedly reduced compared with SHAM-VEH. (*c*) OVX-EST. A dramatic restoration of the apical plasma membrane microprojections and intense label along the apical plasma membrane is evident when compared with OVX-VEH. 19,900×.

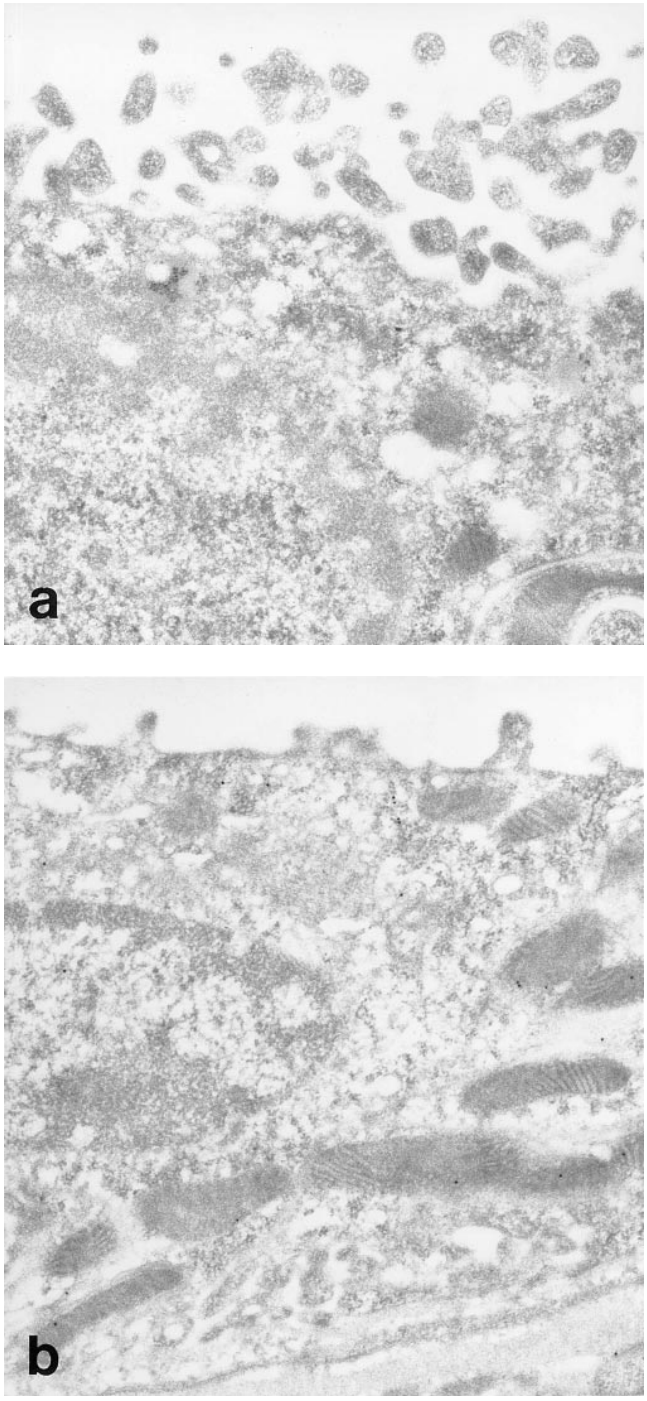

Figure 7. Transmission electron micrographs demonstrating the specificity of the immunogold label in the DCT. (*a*) Apical region of a DCT cell subjected to immunogold labeling with the primary antibody omitted. Only rare gold particles are present. (*b*) Thick ascending limb cell subjected to the immunogold procedure. Occasional gold particles are scattered over the cell. (*a*) 22,200×; (*b*) 18,600×.

gen on the rTSC1. Among these are renin, angiotensin II, glucocorticoids, and calcitonin. Estrogen administration can elevate plasma renin activity and plasma angiotensinogen in rats (10) and humans (3). However, estrogen-induced stimulation of the renin–angiotensin system has only been observed with oral administration, the use of synthetic estrogens, or with high dosages, and has not been observed with parenteral administration of 17β-estradiol in more physiologic dosages similar to the dose and route used in this study (3). Furthermore, even when plasma renin activity, angiotensinogen, and angiotensin II levels are elevated after oral estrogen administration, elevated serum aldosterone levels have not been consistently observed in humans (3) or rats (10). Thus, although evidence suggests that mineralocorticoids increase thiazide-sensitive NaCl transport (11, 12), it is unlikely that aldosterone is responsible for the estradiol-induced increase in rTSC1 in the DCT under the conditions of these experiments. It is also unlikely that regulation of the rTSC1 by ovariectomy and estrogen replacement observed in our study is a direct effect of angiotensin II. Although angiotensin II directly stimulates sodium transport in the rat DCT, the mechanism is by stimulation of Na/H exchange rather than by activation of NaCl uptake by the thiazide-sensitive NaCl cotransporter (13).

However, parenteral physiologic doses of estrogen do increase plasma glucocorticoids in humans (14) and rats (15). Glucocorticoid receptor immunoreactivity has been demonstrated in the DCT (16), and glucocorticoids increase both tritiated metolazone binding in the kidney (11, 12) and thiazide-sensitive NaCl transport in DCT microperfused in vivo (12). Elevation of plasma glucocorticoids also could potentially activate mineralocorticoid receptors, and thus stimulate rTSC1 expression. Although the enzyme 11β-hydroxysteroid dehydrogenase (11β-HSD) typically protects the mineralocorticoid receptor in vivo from activation by the relatively high circulating levels of glucocorticoids, and regulates ligand occupancy of glucocorticoid receptors (17), there is evidence that the known isoforms of this protective enzyme are not present in at least a portion of the distal convoluted tubule (18–20). Thus, it is possible that the effect of estradiol that we observed on the rTSC1 is mediated by elevated glucocorticoids unchecked by 11β-HSD.

A third possible intermediary in rTSC1 regulation in these studies is calcitonin. Ovariectomy reduces basal serum calcitonin levels and the calcitonin response to hypercalcemia (21), and estrogen administration increases calcitonin mRNA expression in the thyroid (22). Furthermore, salmon calcitonin enhances tritiated metolazone binding in renal homogenates, but the same dose of rat calcitonin failed to duplicate this effect (23). Thus, it is doubtful that estrogen stimulation of endogenous calcitonin production and release would be responsible for the effect of ovariectomy and estrogen replacement that we observed on the rTSC1.

It could be postulated that the effect that we observed is simply an adaptation to changes in sodium delivery to the DCT. We believe that this is an unlikely explanation for several reasons. First, we observed a reduction in rTSC1 immunoreactive protein and immunogold label in kidneys of pair-fed OVX rats as well as in OVX rats fed ad libitum. Secondly, in normal animals, changes in dietary sodium do not affect the thiazide receptor density measured by tritiated metolazone binding (24). Furthermore, although an increase in distal sodium delivery may increase renal thiazide receptor density (24), under similar conditions increased distal sodium delivery has been shown to cause an increase in DCT cell size and basolateral plasma membrane (25) rather than the changes in the apical plasma membrane that we observed.

Our findings suggest that ovariectomy and estrogen re-

placement may have significant effects on NaCl transport in the distal convoluted tubule, which may have important clinical implications with respect to renal sodium transport and response to thiazide diuretic treatment, particularly in postmenopausal women or as a contributing factor in fluid balance or hypertension in pregnancy. Furthermore, because pharmacologic inhibition of the thiazide-sensitive NaCl cotransporter enhances calcium reabsorption in the distal convoluted tubule (26, 27), a reduction in TSC expression after ovariectomy or naturally occurring menopause may similarly result in enhanced calcium reabsorption by the distal convoluted tubule.

In summary, we observed that ovariectomy in rats results in a decrease in rTSC1 immunoreactive renal membrane protein and a reduction in the complexity of the apical plasma membrane and the density of immunogold label for rTSC1 in the distal convoluted tubule. In addition, we found that estradiol replacement restores the distal convoluted tubule ultrastructure and rTSC1 label to normal. We conclude that estrogen enhances the density of rTSC1 in the distal convoluted tubule, and thus may alter renal sodium transport by this mechanism.

Acknowledgments

We gratefully acknowledge the technical assistance of Frederick Kopp and Wendy Wilber.

These studies were supported by grants from the American Heart Association, Florida Affiliate (Initial Investigatorship no. 9503007 to J.W. Verlander), the University of Florida Division of Sponsored Research (DSR-D 3400 to J.W. Verlander), and the National Institutes of Health (DK45792 to S.C. Hebert and DK08898 to M.R. Kaplan). T.M. Tran's participation in the University of Florida Student Science Training Program was supported by a grant from the Volusia County Heart Association.

References

1. Christy, N.P., and J.C. Shaver. 1974. Estrogens and the kidney. *Kidney Int.* 6:366–376.

2. Chen, Z., D.A. Vaughn, and D.D. Fanestil. 1994. Influence of gender on renal thiazide diuretic receptor density and response. *J. Am. Soc. Nephrol.* 5: 1112–1119.

3. Oelkers, W.K. 1996. Effects of estrogens and progestogens on the renin-aldosterone system and blood pressure. *Steroids.* 61:166–171.

4. Gesek, F.A., and P.A. Friedman. 1995. Sodium entry mechanisms in distal convoluted tubule cells. *Am. J. Physiol.* 268:F89–F98.

5. Gamba, G., S.N. Saltzberg, M. Lombardi, A. Miyanoshita, J. Lytton, M.A. Hediger, B.M. Brenner, and S.C. Hebert. 1993. Primary structure and functional expression of a cDNA encoding the thiazide-sensitive, electroneutral sodium-chloride cotransporter. *Proc. Natl. Acad. Sci. USA.* 90:2749–2753.

6. Plotkin, M.D., M.R. Kaplan, J.W. Verlander, W.S. Lee, D. Brown, E. Poch, S.R. Gullans, and S.C. Hebert. 1996. Localization of the thiazide sensitive Na-Cl cotransporter, rTSC1 in the rat kidney. *Kidney Int.* 50:174–183.

7. McLean, I.W., and P.K. Nakane. 1974. Periodate-lysine-paraformaldehyde fixative. A new fixative for immunoelectron microscopy. *J. Histochem. Cytochem.* 22:1077–1083.

8. Verlander, J.W., K.M. Madsen, J.H. Galla, R.G. Luke, and C.C. Tisher. 1992. Response of intercalated cells to chloride depletion metabolic alkalosis. *Am. J. Physiol.* 262:F309–F319.

9. Weibel, E.R., and R.P. Bolender. 1973. Stereological techniques for electron microscopic morphometry. *In* Principles and Techniques of Electron Microscopy. M.A. Hayat, editor. Van Nostrand Reinhold Company Ltd., New York. 237–296.

10. Inao, H. 1985. Effects of sex steroid hormones on vascular reactivity to angiotensin II in castrated rat. *Acta Obstet. Gynaecol. Jpn.* 37:2806–2812.

11. Chen, Z., D.A. Vaughn, P. Blakely, and D.D. Fanestil. 1994. Adrenocortical steroids increase renal thiazide diuretic receptor density and response. *J. Am. Soc. Nephrol.* 5:1361–1368.

12. Velazquez, H., A. Bartiss, P. Bernstein, and D.H. Ellison. 1996. Adrenal steroids stimulate thiazide-sensitive NaCl transport by rat renal distal tubules. *Am. J. Physiol.* 270:F211–F219.

13. Wang, T. and G. Giebisch. 1996. Effects of angiotensin II on electrolyte transport in the early and late distal tubule in rat kidney. *Am. J. Physiol.* 271: F143–F149.

14. Mahajan, D.K., R.B. Billiar, M. Jassani, and A.B. Little. 1978. Ethinyl estradiol administration and plasma steroid concentrations in ovariectomized women. *Am. J. Obstet. Gynecol.* 130:398–402.

15. Burgess, L.H., and R.J. Handa. 1992. Chronic estrogen-induced alterations in adrenocorticotropin and corticosterone secretion, and glucocorticoid receptor-mediated functions in female rats. *Endocrinology.* 131:1261–1269.

16. Farman, N., M.E. Oblin, M. Lombes, F. Delahaye, H.M. Westphal, J.P. Bonvalet, and J.M. Gasc. 1991. Immunolocalization of gluco- and mineralocorticoid receptors in rabbit kidney. *Am. J. Physiol.* 260:C226–C233.

17. Whorwood, C.B., J.A. Franklyn, M.C. Sheppard, and P.M. Stewart. 1992. Tissue localization of 11 beta-hydroxysteroid dehydrogenase and its relationship to the glucocorticoid receptor. *J. Steroid Biochem. Mol. Biol.* 41:21–28.

18. Kapturczak, M. 1994. Heterogenitat der 11β-hydroxysteroid-dehydrogenase-aktivitat entlang des nephrons von ratte und maus: mikrobiochemische und immunhistochemische untersuchungen. 1–36.

19. Rundle, S.E., J.W. Funder, V. Lakshmi, and C. Monder. 1989. The intrarenal localization of mineralocorticoid receptors and 11 beta-dehydrogenase: immunocytochemical studies. *Endocrinology.* 125:1700–1704.

20. Ellison, D.H., M. Bostanjoglo, H. Velazquez, R.F. Reilly, S. Kunchaparty, W.B. Reeves, and S. Bachmann. 1996. Electroneutral Na-Cl cotransport and Na/Ca exchange in mineralocorticoid target cells. *J. Am. Soc. Nephrol.* 7(Abstr.):1279.

21. Cressent, M., Z. Bouizar, E. Pidoux, M.S. Moukhtar, and G. Milhaud. 1979. Effet de l'ovariectomie sur le taux de calcitonine plasmatique chez le rat. *Comp. Rend. Acad. Sci. Paris Serie D.* 289:501–504.

22. Naveh Many, T., G. Almogi, N. Livni, and J. Silver. 1992. Estrogen receptors and biologic response in rat parathyroid tissue and C cells. *J. Clin. Invest.* 90:2434–2438.

23. Blakely, P., D.A. Vaughn, and D.D. Fanestil. 1996. Effects of calcium-modulating hormones on thiazide receptor density. *J. Am. Soc. Nephrol.* 7: 1052–1057.

24. Chen, Z., D.A. Vaughn, K. Beaumont, and D.D. Fanestil. 1990. Effects of diuretic treatment and of dietary sodium on renal binding of ^{3}H-metolazone. *J. Am. Soc. Nephrol.* 1:91–98.

25. Kaissling, B., and B.A. Stanton. 1988. Adaptation of distal tubule and collecting duct to increased sodium delivery. I. Ultrastructure. *Am. J. Physiol.* 255:F1256–F1268.

26. Costanzo, L.S. 1985. Localization of diuretic action in microperfused rat distal tubules: Ca and Na transport. *Am. J. Physiol.* 248:F527–F535.

27. Gesek, F.A., and P.A. Friedman. 1992. Mechanism of calcium transport stimulated by chlorothiazide in mouse distal convoluted tubule cells. *J. Clin. Invest.* 90:429–438.